Scanning Microscopy

Volume 2 | Number 2 Article 15

2-6-1988

Recovery of Semiconductor and Defect Properties from Charge-Collection Measurements

C. Donolato
CNR-Instituto LAMEL

Scanning Microscopy, Vol. 2, No. 2, 1988 (Pages 801-811) 0891-7035/88$3.00+.00
Scanning Microscopy International, Chicago (AMF O'Hare), IL 60666 USA

RECOVERY OF SEMICONDUCTOR AND DEFECT PROPERTIES FROM CHARGE-COLLECTION MEASUREMENTS

C. Donolato

CNR-Istituto LAMEL, Via Castagnoli 1, 40126 Bologna, Italy

(Received for publication April 06, 1987, and in revised form February 06, 1988)

Abstract

This paper discusses the modeling of the measurements which are performed with the charge-collection, or Electron Beam Induced Current (EBIC) technique of the scanning electron microscope, and the use of the related theoretical results for recovering bulk and local recombination properties of semiconductors. A general description of different EBIC measurements can be given on the basis of the notion of charge-collection probability $\varphi(\underline{r})$ in the device being examined. This function can be calculated by solving a stationary diffusion equation and the induced current results from the convolution of $\varphi(\underline{r})$ with the generation function of the electron beam. According to this approach, EBIC experiments give information about φ or the essential semiconductor or defect parameters upon which φ is dependent. The more usual procedures to recover this information from actual measurements are reviewed and some new possibilities are examined.

KEY WORDS: Charge Collection, Electron Beam Induced Current, Carrier Recombination, Diffusion Length, Crystal Defects, Semiconductor Characterization, Image Contrast.

Phone No. 051 - 287011

Introduction

The basic principles and applications of the charge-collection, or Electron Beam Induced Current (EBIC) technique of the scanning electron microscope have been reviewed in a number of papers (see, e.g.,(Hanoka and Bell, 1981),(Leamy, 1982), (Holt and Lesniak, 1985)). This paper focusses the attention on the problem of recovering quantitative information on bulk or local recombination properties of semiconductors from EBIC measurements; no attempt will be made of including all configurations and models which have appeared in the literature.

The aim of this paper is rather that of giving a common description of the more usual steady-state EBIC experiments and to show the connection between the different methods used to evaluate the results. This attempt of generalization relies on the notion of charge-collection probability, i.e. the probability $\varphi(\underline{r})$ that a minority carrier generated at $\underline{r}$ will be collected and contribute to the induced current (Possin and Kirkpatrick, 1979). The SEM electron beam probes this local device property by injecting carriers over a definite region (the generation volume) and the induced current represents a weighted average of φ over this region.

Having introduced φ as the fundamental device property for EBIC experiments, it is relevant to show how φ can be calculated both in a perfect semiconductor and in the presence of defects, and to discuss the different methods suitable for recovering φ (or the essential semiconductor parameters contained in φ) from the measured induced current. These points will be examined here by often making reference to specific examples for clarity of the discussion.

Evaluation of the induced current

Let us consider the configuration of Fig.1, where the junction plane is assumed to be coincident with the surface of the semiconductor and the beam excitation is represented by a unit point source of carriers at a depth z_0. The usual method to evaluate the collected current is to first solve the diffusion equation for the excess minority carrier density $p(\underline{r})$, with suitable boundary conditions, and then evaluate the integral of the diffusion current density over the

List of symbols

A	area of the contrast profile (cm)
c	contrast
D	minority-carrier diffusion coefficient ($cm^2 s^{-1}$)
$e(\underline{r})$	unit function
E	electron beam energy (eV)
$g(\underline{r})$	generation rate of the e-h pairs per unit volume ($cm^{-3} s^{-1}$)
g_o	total generation rate (s^{-1})
$G(\underline{r},\underline{r}_o)$	three-dimensional Green's function (cm^{-3})
G_2	two-dimensional Green's function (cm^{-2})
G_1	one-dimensional Green's function (cm^{-1})
h(z,E)	depth distribution of the e-beam generation (cm^{-1})
i*(x)	contrast profile
I	(particle) induced current (s^{-1})
I_o	background current (s^{-1})
I*	defect signal (s^{-1})
k(x,z,E)	two-dimensional distribution of the e-beam generation (cm^{-2})
L	minority-carrier diffusion length (cm)
$\Lambda(z/R)$	Everhart and Hoff's polynomial
$m(z_o)$	first moment of φ (cm^2)
$\underline{r}$	position vector (cm)
$\underline{r}_o$	position vector of the point source (cm)
R	primary electron range (cm)
s	surface recombination velocity (cm s^{-1})
S	reduced surface recombination velocity (cm^{-1})
t	metallization thickness
v(t)	auxiliary function (cm^{-1})
w	correction factor
W	depletion layer width (cm)
x,y,z	spatial coordinates (cm)
$\bar{z}$	center of gravity of the depth-dose function (cm)
α	inclination angle
γ	recombination strength of a volume defect (s^{-1})
γ_s	recombination strength of a surface defect (cm s^{-1})
γ_d	recombination strength of a line defect ($cm^2 s^{-1}$)
γ_p	recombination strength of a point-like defect ($cm^3 s^{-1}$)
$\delta(\underline{r})$	Dirac delta function (cm^{-3})
ε	dislocation radius (cm)
η	charge-collection efficiency
σ	standard deviation of the contrast profile (cm)
τ, τ'	minority carrier lifetimes (s)
φ	charge-collection probability

junction plane. If D is the minority carrier diffusion coefficient, τ their lifetime and $L=(D\tau)^{\frac{1}{2}}$ the diffusion length, we get the equation:

$$\nabla^2 p(\underline{r}) - (1/L^2)\, p(\underline{r}) = -(1/D)\,\delta(\underline{r} - \underline{r}_o) \quad (1)$$

where the delta-function term describes the point generation at $\underline{r}_o$. The boundary conditions are:

$$p(x,y,0) = 0 \; ; \quad p \to 0 \quad \text{for} \quad r \to \infty. \quad (2)$$

In this simple case the solution, which is also the Green's function $G(\underline{r},\underline{r}_o)$ of the problem, can be written down immediately using the method of images (Morse and Feshbach, 1953):

$$p(\underline{r}) = G(\underline{r},\underline{r}_o) = [(1/r_1)\exp(-r_1/L) - (1/r_2)\exp(-r_2/L)]\,/(4\pi D) \quad (3)$$

where $r_1 = |\underline{r} - \underline{r}_o|$, $r_2 = |\underline{r} - \underline{r}'_o|$, $\underline{r}_o$ and $\underline{r}'_o$ being the position of the source and its image in the plane z=0, respectively. The collected particle

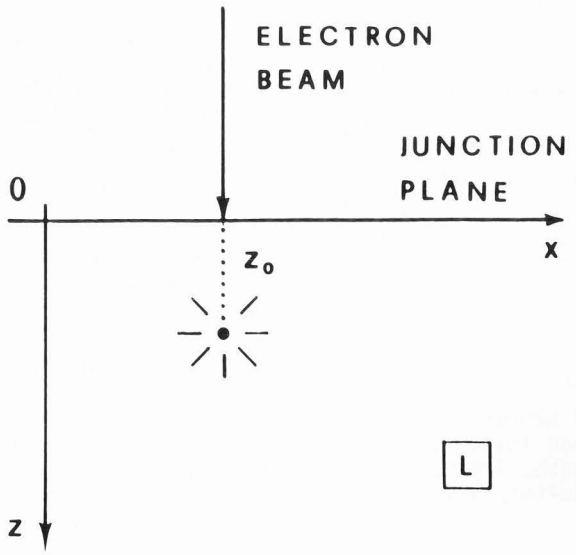

Figure 1: Point generation in a semi-infinite semiconductor.

current is given by:

$$\varphi(\underline{r}_0) = D \int_{-\infty}^{+\infty}\int_{-\infty}^{+\infty} \left.\frac{\partial G}{\partial z}\right|_{z=0} dx\, dy \qquad (4)$$

The double integration can be performed easily by using cylindrical coordinates about the beam axis and yields a result independent of x_0, y_0

$$\varphi(z_0) = \exp(-z_0/L) \qquad (5)$$

This function represents the charge-collection probably in the structure, since for a point source of arbitrary strength, φ also gives the fraction of the injected charge that is collected by the junction.

The well-known simple result of Eq.(5) raises the question whether it was really necessary to solve first Eq.(1) for $p(\underline{r})$ to obtain the single-variable function $\varphi(z_0)$. Actually the result of Eq.(5) could have been obtained directly by using a reciprocity theorem analogous to the Green's reciprocation theorem of electrostatics (see e.g., Jackson, 1975).

The theorem states that the diffusion current produced by a unit point source at $\underline{r}_0$ is the same (apart from the dimensions) as the value at $\underline{r}_0$ of the minority carrier density due to a unit density of carriers at the junction edge (Donolato, 1985a). This latter problem requires solving the one-dimensional equation:

$$\varphi''(z) - (1/L^2)\,\varphi(z) = 0 \qquad (6)$$

with the boundary conditions:

$$\varphi(0) = 1 \quad ; \quad \varphi(\infty) = 0 \qquad (7)$$

The solution of Eq.(6) with Eq.(7) is straightforward and is just given by Eq.(5).

This simple example illustrates the advantage of treating a charge-collection problem in terms of charge-collection probability, since this function has a close relation (see later) to the measured current and can be easier to calculate than the non-observable minority carrier density. A formal proof of the reciprocity theorem is given in (Donolato, 1985a); extensions of the theorem are discussed by (Misiakos and Lindholm, 1985).

If the beam excitation is described more realistically by a three-dimensional distribution $g(\underline{r})$ [$cm^{-3}s^{-1}$], the collected current is obtained by adding the contributions of the elementary volumes of the generation region; this procedure is justified by the linearity of Eq.(1), even for spatially varying lifetime. Hence,

$$I = \int_V \varphi(z)\, g(\underline{r})\, d\underline{r} = \int_0^{\infty} dz\, \varphi(z) \int_{-\infty}^{+\infty}\int_{-\infty}^{+\infty} g(\underline{r})\, dx\, dy \qquad (8)$$

The integration of g over x,y yields the depth distribution of the generation, hence we see that I does not depend on the lateral distribution of g (Hackett, 1972). This is a consequence of the fact that φ is only dependent on z (and not on x, y); this property results from the physical invariance of the structure of Fig.1 for translations along x,y.

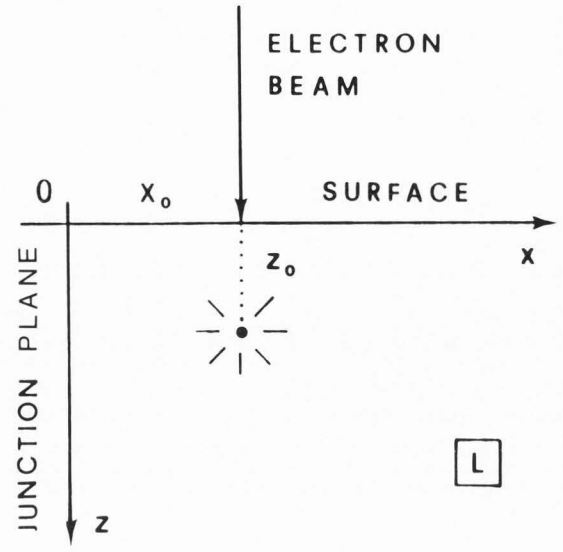

Figure 2: Point generation and normal collector: the junction plane is perpendicular to the irradiated surface.

If g_0 [s^{-1}] is the total generation rate and h(z,E) is the normalized (energy dependent) depth distribution of the generation, Eq.(8) can be written as:

$$I(E) = g_0 \int_0^{\infty} \varphi(z)\, h(z,E)\, dz \qquad (9)$$

The ratio $I(E)/g_0$ represents the fraction of the total injected charge that is collected by the junction and is called charge collection efficiency η of the device. Thus:

$$\eta(E) = \int_0^{\infty} \varphi(z)\, h(z,E)\, dz \qquad (10)$$

Since h(z,E) is to be regarded as known, the measurement of $\eta(E)$ yields information about $\varphi(z)$; methods for recovering this information will be discussed in the next section.

In a less symmetric experimental configuration, as in the normal-collector geometry of Fig.2, φ becomes a function both of x and z, hence the distribution of g along x (but not along y) becomes also relevant. If $k(x-x_0,z,E)$ is the normalized projection of g onto the xz plane, $x_0 \geqslant 0$ being the beam position, the induced current becomes:

$$I(x_0,E) = g_0 \int_{-\infty}^{+\infty}\int_0^{\infty} \varphi(x,z)\, k(x-x_0,z,E)\, dx\, dz \qquad (11)$$

Recovering $\varphi(x,z)$ from $I(x_0,E)$ becomes more difficult, and actually in this case a number of approximations have been introduced. Equation (11) also holds for the planar collector geometry,

where the beam is incident normal to a Schottky diode (or a shallow p-n junction) and moved away from the diode edge (Ioannou, 1980).

Reconstruction of the charge-collection probability

Generally the form of the function φ to be reconstructed from EBIC data is specified a priori from a model of the structure being investigated. Thus φ will have a definite dependence upon space variables and some additional parameters, which are related to the configuration and recombination properties of the semiconductor. Reconstructing the function φ thus specified means, more restrictively, determining the values of these parameters (e.g., diffusion length, surface recombination velocity). However, it will be shown that in a simple one-dimensional case φ can be determined without making any assumption about its form.

One dimension

Let us consider for definiteness the case of collection efficiency measurements on Schottky diodes (Wu and Wittry, 1978). The appropriate model function $\varphi(z)$ contains as free parameters the thickness t of the metallization, the width W of the depletion layer and the values L of the bulk diffusion length of the semiconductor. It is assumed that $\varphi=0$ for $0 \leqslant z < t$, $\varphi=1$ for $t \leqslant z < t+W$ and $\varphi = \exp[-(z-t-W)/L]$ for $z \geqslant t+W$ (Fig.3). Thus, according to Eq.(10), the measured value of η at the beam energy E_i can be expressed as:

$$\eta_i = \eta(t,W,L,E_i) \qquad i = 1,\ldots N \qquad (12)$$

The three parameters t,W,L, or those of them that are not known, are estimated by a least-squares fitting, in general non-linear, of the function η to the N measured values. With proper changes, the method has been adapted to the evaluation of minority carrier diffusion length and surface recombination velocity of the emitter of n-p diodes (Possin and Kirkpatrick, 1979).

It has been observed, however, that the integral equation (10) specifies uniquely $\varphi(z)$, in the depth range explored by the electron beam, without any explicit knowledge of the device structure (Possin and Kirkpatrick, 1979). A closed-form inversion formula for φ has been derived in the case of silicon on the basis of the following considerations (Donolato, 1986a).

For silicon, the depth-dose function h(z,E) can be expressed through a cubic polynomial Λ of the normalized depth z/R, R=R(E) being the Grün range of primary electrons (Everhart and Hoff, 1971). Thus Eq.(10) becomes:

$$\eta(R) = (1/R) \int_0^{1.1\,R} \varphi(z)\ \Lambda(z/R)\ dz \qquad (13)$$

since for $z > 1.1\ R$ $\Lambda = 0$ (Everhart and Hoff, 1971). With a simple change of variables, Eq.(13) can be given the standard form of a Volterra integral equation of the first kind (Donolato, 1986a). The special polynomial form of the kernel allows Eq.(13) to be converted into an equivalent differential equation, which turns out to be solvable in closed form. The solution is given explicitly in (Donolato, 1986a) and has the form:

$$\varphi(z) = F(z, \eta, \eta', \eta'') \qquad (14)$$

where η' and η'' are the first and second derivative of η, respectively. Such an equation allows in principle the direct reconstruction of φ from $\eta(E)$ data. Its practical use, however, requires obtaining a good estimate of η', η'' from actual noisy experimental data, and has not yet been attempted.

Two dimensions

For the evaluation of experimental EBIC scans, Eq.(11) has been generally simplified by replacing the extended generation with a point source at a depth $z_0(E)$. Thus, for the configuration of Fig.2 the model function has the form:

$$I(x_0,E) = g_0\, \varphi(x_0, z_0(E), s, L) \qquad (15)$$

where the semiconductor parameters s (surface recombination velocity) and L have been indicated explicitly. Numerical evaluations comparing $\varphi(x_0, z_0)$ for a point source and extended sources of various shapes indicate that the point source approximation is adequate (Luke et al., 1985). However, generations along a line (Oelgart et al., 1981) or over a volume (Fuyuki et al., 1980) have also been considered.

There may be some uncertainty about the choice of z_0; for silicon, possible choices are $z_0 = 0.3\ R$, which corresponds to the maximum of the depth-dose function, or $z_0 = 0.5\ R$, corresponding to the center of the uniform generation sphere approximating the generation volume. However, as suggested by Berz and Kuiken (1976), the most appropriate choice is the center of gravity $\bar{z}$ of the depth-dose function; for the Everhart

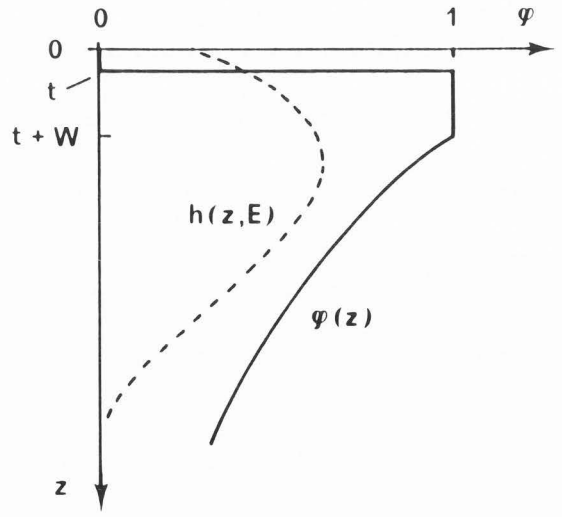

Figure 3: Electron beam depth-dose function h(z,E) (arbitrary units) and charge collection probability $\varphi(z)$ in a Schottky diode.

and Hoff's function, $\bar{z} = 0.41\ R$. An analytical argument for this choice is given by (Donolato, 1983a).

Even with the point source approximation, $I(x_0,z_0) \propto \varphi(x_0, z_0)$ has a rather complicated integral representation (Berz and Kuiken, 1976), (Donolato, 1983a), (Luke et al., 1985), so that asymptotic approximations for large x_0 have been derived. Thus Berz and Kuiken (1976) show that for $x_0 \gg L$ and $z_0 \ll L$

$$I(x_0) \propto \begin{cases} \exp(-x_0/L) & s = 0 \\ (x_0/L)^{-\frac{1}{2}} \exp(-x_0/L) & s = \infty \end{cases} \qquad (16)$$

These simple relations are the basis of a well-known method of determining L by analyzing the asymptotic slope of $I(x_0)$ in a logarithmic plot, but are useful only if it is known a priori that s is either very low or very high. If this information is not available, s and L can be determined simultaneously by fitting the exact expression for $I(x_0,z_0)$ to experimental scans (at least two) taken at different beam energies (Oelgart et al., 1981).

A different method of evaluating simultaneously s and L relies on an integral property of the exact expression of $\varphi(x_0,z_0)$, i.e. its first moment about $x_0 = 0$

$$m(z_0) = \int_0^\infty \varphi(x_0,z_0)\ x_0\ dx_0 \qquad (17)$$

which has the simple expression, with $S = s/D$

$$m(z_0) = L^2 \left[1 - \frac{SL}{1 + SL} \exp(-z_0/L) \right] \qquad (18)$$

By evaluating m for two scans at different beam energies (i.e. for two values of z_0), S and L can be determined uniquely; details on the application of this method are given in (Donolato, 1983a).

The case of the planar collector geometry has been treated by Ioannou and Dimitriadis (1982), Kuiken and van Opdorp (1985), and Donolato (1985b). The asymptotic expressions for $I(x_0)$ become in this case:

$$I(x_0) \propto \begin{cases} (x_0/L)^{-1/2} \exp(-x_0/L) & s = 0 \\ (x_0/L)^{-3/2} \exp(-x_0/L) & s = \infty \end{cases} \qquad (19)$$

Ioannou and Dimitriadis (1982) analyze some experimental scans using Eq.(19) for $s = \infty$; Kuiken and van Opdorp discuss the simultaneous determination of s and L on the basis of more general asymptotic expansions valid for any s. An alternative method for determining L (but not directly s) uses the variance σ^2 of the derivative of the normalized profile $I'(x_0)$ (Donolato, 1985b):

$$\sigma^2 = 1/2\ w\ L^2 + L\ z_0 \qquad (20)$$

where w is a factor dependent on s with $0 \leqslant w \leqslant 1$. By evaluating σ^2 for two profiles at different beam energy (i.e. different values of z_0) and taking the difference it is possible to determine L without any assumption on the value of s.

Determination of depth-dependent diffusion length

In the examples discussed so far, the bulk recombination in the semiconductor has been described by a constant diffusion length L. However, there are relevant practical cases where L varies with the depth, for instance as a consequence of gettering or passivation treatments.

The change with the depth of semiconductor properties (for instance the defect density) is often studied by inspection with the optical microscope of angle-beveled samples. This kind of samples can be adapted to EBIC studies by forming a Schottky barrier collector on the beveled surface (Fig.4) (Kittler and Schröder, 1983), (Nauka et al., 1986).

Fig.5a is the EBIC micrograph obtained by this technique on an instrinsically gettered silicon sample; the horizontal axis is labelled with the depth z in the sample, which is related to the beam position x on the bevel by the relation $x = z \sin\alpha$. The image shows that the treatment has produced a defect-free denuded zone about 15 μm thick on a defect-rich bulk; the stacking faults observed on the unbeveled surface ($z < 0$) were produced by an oxidation following the gettering process. Figure 5b shows the corresponding collection efficiency profile, obtained by scanning the sample on a line along x and recording the induced current; the current values have been converted into collection efficiency values $\eta(z)$ by normalization to the total generation rate (see Eqs.(9), (10)).

The problem is to recover from the measured $\eta(z)$ a diffusion length profile L(z), which represents an average value including both bulk and defect recombination. For each position x' of the beam on the bevel, the sample can be considered as being delimited by the plane $z = z' = x' \sin\alpha$, so that the scheme of Fig.1 can be applied. The equation for the charge collection probability

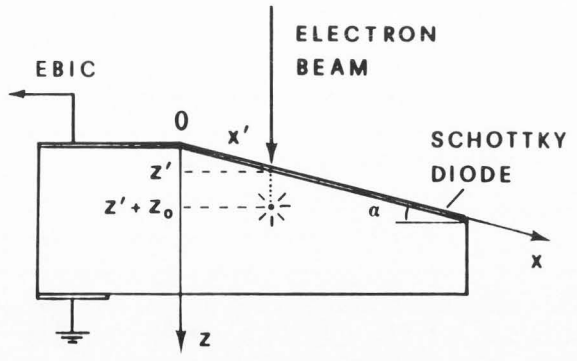

Figure 4: Schematic of EBIC observations in angle lapped specimens. The actual value of α is about 3°.

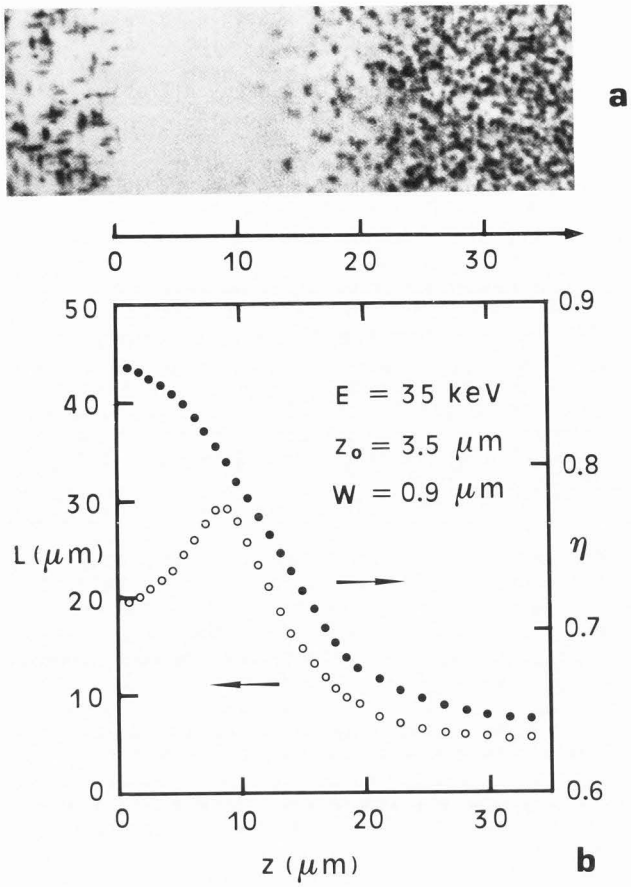

Figure 5: (a) EBIC micrograph taken at 25 keV of an intrinsically gettered silicon sample, using the arrangement of Fig.4. (b) Measured collection efficiency profile (•) and reconstructed diffusion length profile (○).

$\varphi(z,z')$ is now:

$$\varphi'' - [1/L^2(z)]\varphi = 0 \qquad (21)$$

with the boundary conditions similar to those of Eq.(7):

$$\varphi(z',z') = 1 \qquad (22.1)$$

$$\varphi(\infty,z') = 0 \qquad (22.2)$$

Let us write φ in the form:

$$\varphi(z,z') = \exp\left[-\int_{z'}^{z} v(t)\,dt\right] \qquad (23)$$

which satisfies automatically (22.1) and also (22.2), since typically $v(t) \geqslant v_0 > 0$. Substitution of this expression into Eq.(21) yields an equation for v(z):

$$v^2(z) - v'(z) = 1/L^2(z) \qquad (24)$$

which cannot be solved in close form (nor could Eq.(21)), but does provide the required link between $\eta(z)$ and L(z). In fact, according to the point source approximation, the charge collection efficiency is given by:

$$\eta(z') = \varphi(z' + z_0, z') \qquad (25)$$

where z_0 is the depth of the point source. Using the expression (23) for φ yields:

$$\eta(z') = \exp\left[-\int_{z'}^{z'+z_0} v(t)\,dt\right]$$

$$\simeq \exp\left[-z_0 v(z' + z_0/2)\right] \qquad (26)$$

This equation specifies v(z') (for $z' \geqslant z_0/2$) in terms of the measured profile $\eta(z')$; substitution of v into Eq.(24) yields L(z).

The reconstructed L(z) profile shown in Fig.5b was obtained by this method. It is interesting to note that the decrease of L near the surface correlates well with the presence of the surface stacking faults visible in Fig.5a. It is possible to refine the model by including the presence of the depletion layer and the finite extension of the generation volume; for details the reader is referred to (Donolato and Kittler, 1987).

The EBIC contrast of defects

The reciprocity theorem introduced with Eq.(6) also holds if the minority-carrier lifetime is position-dependent, and therefore is useful for treating charge-collection in the presence of semiconductor defects. Thus, by representing a defect as a region F where the lifetime τ' (assumed to be constant, for simplicity) is smaller than the bulk lifetime τ, we obtain the equation for $\varphi(\underline{r})$:

$$\nabla^2\varphi(\underline{r}) - (\gamma/D)e(\underline{r})\varphi(\underline{r}) - (1/L^2)\varphi(\underline{r}) = 0 \qquad (27)$$

where $L = (D\tau)^{\frac{1}{2}}$, $\gamma = (1/\tau' - 1/\tau)$, $e(\underline{r}) = 1$ inside F and vanishes elsewhere. For the configuration of Fig.1 the boundary conditions are:

$$\varphi(x,y,0) = 1 \;; \quad \varphi(\underline{r}) = 0\,,\ r \to \infty \qquad (28)$$

The factor $\gamma\,[s^{-1}]$ represents the recombination strength of the defect. The definition given here differs from that given previously (Donolato, 1978/79), (Donolato, 1979) by a factor of D, but has the advantage that the strength of a surface-like defect gets the usual dimensions of a surface recombination velocity (see later).

Equation (27) can be solved approximately by treating the term containing γ as a perturbation. Writing $\varphi = \varphi_0 + \varphi_1$ with $\varphi_1 \ll \varphi_0$, we see that φ_0 satisfies:

$$\nabla^2\varphi_0(\underline{r}) - (1/L^2)\varphi_0(\underline{r}) = 0; \quad \varphi_0(x,y,0) = 1 \qquad (29)$$

which is solved by $\varphi_0(\underline{r}) = \varphi_0(z) = \exp(-z/L)$. The first order correction then obeys:

$$\nabla^2\varphi_1(\underline{r}) - (1/L^2)\varphi_1(\underline{r}) = (\gamma/D)e(\underline{r})\exp(-z/L) \qquad (30)$$

with

$$\varphi_1(x,y,0) = 0 \qquad (31)$$

Eq.(30) is just Eq.(1) with an extended sink term; the pertinent Green's function is that of Eq.(3), hence:

$$\varphi(\underline{r}) = \varphi_0 + \varphi_1 = \exp(-z/L) - \gamma \int_F \exp(-z'/L) G(\underline{r},\underline{r}') d\underline{r}' \qquad (32)$$

This expression represents the first-order approximation to the charge-collection probability in the configuration of Fig.1 with a defect added. We see that the presence of the defect reduces the original probability of Eq.(5), and the magnitude of this reduction, according to the structure of $G(\underline{r},\underline{r}')$, increases by approaching the defect (Fig.6).

If the defect can be approximated by a surface, the volume integral of Eq.(30) can be replaced by a surface integral, provided that γ is replaced by $\gamma_s[\mathrm{cm\ s^{-1}}]$, which can be interpreted as a surface recombination velocity. For a line defect, e.g. a dislocation, the integral is along a line and γ becomes $\gamma_d[\mathrm{cm^2 s^{-1}}]$ (line recombination velocity). In the case of a point-like defect no integration is required and γ becomes γ_p $[\mathrm{cm^3 s^{-1}}]$.

The collected current produced by an electron beam generation $g(\underline{r})$ is given by (see Eq. (8)):

$$I = \int_V g(\underline{r}) \exp(-z/L) d\underline{r} - \gamma \int_F d\underline{r}' \exp(-z'/L) \int_V g(\underline{r}) G(\underline{r},\underline{r}') d\underline{r} \qquad (33)$$

$$= I_0 + I^*$$

This equation describes the EBIC image of a defect as the sum of the background current I_0 and the (negative) defect signal I^*; the image contrast is then given by $i^* = |I^*|/I_0$. Equation (33) reproduces the expression derived previously (Donolato, 1978/79), since the integral over V just gives the distribution $p(\underline{r})$ of beam-injected minority carriers. The present approach, however, separates more clearly the calculation of $\varphi(\underline{r})$, which is a device property, from that of I, which results from the sampling of $\varphi(\underline{r})$ with an external excitation $g(\underline{r})$.

The calculations outlined above represent a first-order approximation (i^* is proportional to γ) to the EBIC contrast of defects, but turns out to give a satisfactory description of observed images (Donolato, 1979). For defect-device configuration of special symmetry, higher-order contributions to the contrast have been calculated (Pasemann, 1981), and in some instances an exact calculation of the contrast has been possible (Donolato, 1983b), (Pasemann, 1986).

Determination of defect properties

Obtaining a value for the recombination strength of a defect from EBIC contrast measurements is a more difficult problem than characterizing homogeneous semiconductors, since defect configuration and recombination parameters of the host semiconductor constitute additional unknown properties.

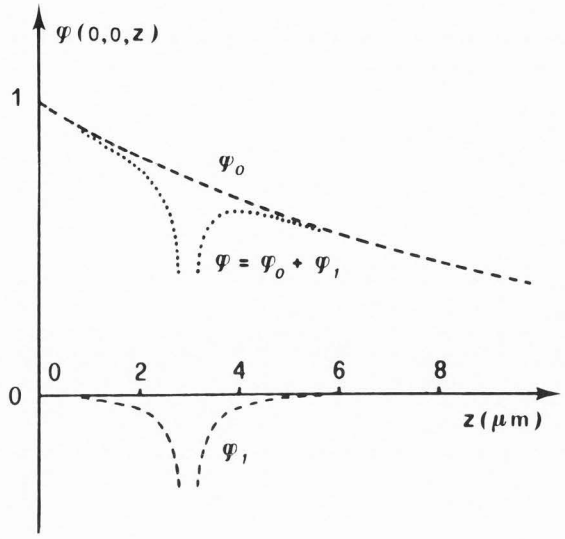

Figure 6: Charge collection probability in the configuration of Fig.1 in the presence of a point-like defect. The plot shows a value of φ along the line through the defect normal to the surface; z' = 3 μm, L = 10 μm, γ/D = 0.8 μm.

For the configuration of Fig.1, the contrast distribution of the image of a defect can be calculated using Eq.(33), if the defect geometry and the semiconductor diffusion length are known. Since in the linear approximation the contrast is proportional to γ, a comparison between the maximum calculated contrast and the observed one yields the value of γ.

This method has been used by Pasemann et al. (1982) for characterizing the activity of dislocations lying parallel to the surface in the emitter of a diode, taking into account additionally higher-order corrections to γ_d. Lifetime and surface recombination velocity of the emitter were determined by energy-dependent collection efficiency measurements, while the dislocation depth was established by transmission electron microscopy (TEM). Defect depth determination by TEM was also used by Kittler et al. (1984) to characterize the recombination strength of circular stacking faults parallel to the surface.

Theoretical computations (Donolato, 1978/79) indicate that the dependence on the beam energy of the contrast of a point-like defect bears information on the defect depth. This property has been used by Mil'vidskii et al. (1985) for determining simultaneously the strength γ_p and the depth z' of point-like defects; the expression of the contrast has the form:

$$c = i^*(0) = \gamma_p F(R(E),z',L) \qquad (34)$$

After having determined L, Mil'vidskii et al. measured c at different values of E; according to

Eq.(34), each couple of values c,E specifies a function $\gamma_p(z')$. The resulting family of curves in the (γ_p,z') plane intersected in a small region of this plane, thereby defining (with some inherent error) the value of both γ_p and z'.

The determination of the defect depth and the related calculation of the geometrical factor F of Eq.(32) can be avoided, if the specification of relative values of γ is sufficient. This feature was used by Ourmazd et al. (1983) for studying the temperature dependence of the strength of dislocations parallel to the surface of the sample. For this configuration, a relation of the form of Eq.(34) holds; therefore, if L is temperature independent, the ratio of the contrast values of a dislocation at two different temperatures equals the ratio of the corresponding strengths. Thus the temperature dependence of γ_d can be studied without determining γ_d itself. The main conclusion of this study was that the temperature-dependent behaviour of the contrast could not be explained in the framework of the linear contrast model. This conclusion has been shown not to be well-founded (Donolato, (1986b), and actually subsequent studies on the same subject went back to the linear model (Wilshaw and Booker, 1985).

Use of integral properties of the image

When the defect configuration has special symmetry (e.g., a straight dislocation either parallel or perpendicular to the sample surface; a plane grain boundary normal to the surface), the EBIC image is completely described by a single line scan through the defect. In this case, the image contrast has been usually characterized by i*(0). Another possibility is to use the area A [cm] of the contrast profile:

$$A = \int_{-\infty}^{+\infty} i^*(x)\, dx \qquad (35)$$

which represents the integral influence of the defect on the collected current (Fig.7). The evaluation of A is a rather straightforward matter, if a digital acquisition system is connected to the SEM.

The profile area has over the maximum contrast i*(0) some advantages, which will be illustrated in the specific case of a straight dislocation parallel to the y axis, located at (x' = 0, z') in the structure of Fig.1. For this geometry, Eq.(30) yields:

$$\varphi_1(x,z) = -\gamma_d \exp(-z'/L)\, G_2(x,z;0,z') \qquad (36)$$

where G_2 is the two-dimensional Green's function resulting from the integration of G along y. If $k(x-x_0,z)$ is the projection of $g(\underline{r})$ onto the plane x,z, we obtain from Eq.(33):

$$i^*(x_0) = \frac{\gamma_d}{I_0} \exp(-z'/L) \int_0^{\infty} dz \int_{-\infty}^{+\infty} k(x-x_0,z) G_2(x,z;0,z')\, dx \qquad (37)$$

By integrating over x_0 we obtain

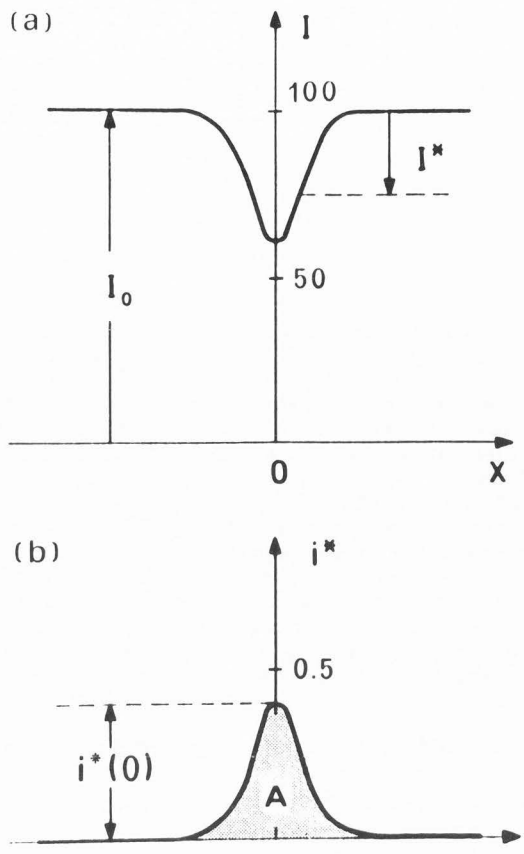

Figure 7: (a) Induced current profile (arbitrary units); (b) corresponding contrast profile $i^* = |I^*|/I_0$.

$$A = \frac{\gamma_d}{I_0} \exp(-z'/L) \int_0^{\infty} h(z)\, G_1(z,z')\, dz \qquad (38)$$

since the integration of k over x_0 produces the depth-dose function h(z), and the integration of G_2 over x yields the one-dimensional Green's function G_1. By solving a simple one-dimensional diffusion equation it is easy to show that (Hackett, 1972):

$$G_1(z,z') = \tfrac{1}{2}(L/D)\{\exp[-|z-z'|/L] - \exp[-(z+z')/L]\} \qquad (39)$$

Eq.(38) shows that A is obtained by integrating the product of the one-variable functions h and G_1; calculating i*(0) would require a double integration of the product of the two-variable functions k and G_2. Hence we see that the additional effort required for evaluating the experimental value of A is compensated by the simpler evaluation of its theoretical value. A further useful property of A, following from Eq.(38), is its independence of the lateral distribution of the generation (e.g., of the beam spot size), as long as the recombination mechanism is linear.

The contrast profile area has been used by

Donolato (1983b) for determining the value of γ_s of a grain boundary; in this case, an additional integral property of the contrast profile, the standard deviation σ, could be related to the bulk diffusion length L. For a dislocation, however, σ is expected to be less sensitive to L than for a grain boundary, because of the one- vs two-dimensional extension; consequently, determining L through σ may prove not to be feasible.

As a second example illustrating another useful property of A, let us consider a plane grain boundary tilted by an angle α from the position perpendicular to the sample surface. The loss of symmetry along x makes an exact solution of the related diffusion problem rather difficult, therefore the properties of A are examined for the first-order approximation to the contrast.

From Eq.(32), it is easy to deduce by integration along the trace of the grain boundary in the x,z plane that:

$$\varphi_1(x,z;\,)=-\gamma_s\int_0^\infty \exp(-z'/L)G_2(x,z;z'\mathrm{tg}\alpha,z')dz'/\cos\alpha \qquad (40)$$

Using Eq.(33), and taking into account that G_2 depends on x and x' only through their difference, we obtain:

$$A(\alpha)=(1/\cos\alpha)\left[\frac{\gamma_s}{I_o}\int_0^\infty dz\; h(z)\int_0^\infty \exp(-z'/L)G_1(z,z')dz'\right] \qquad (41)$$

The term in the square brackets gives A(0), i.e., the values of A for a normal grain boundary; hence Eq.(41) can be rewritten simply as:

$$A(\alpha) = A(0)/\cos\alpha \qquad (42)$$

Therefore, although an inclination of α from the normal position modifies symmetry, maximum value and area of the contrast profile of a grain boundary, the product $A\cdot\cos\alpha$ remains unaffected. This property can be useful in comparing the activity of grain boundaries with different inclination. It must be remembered, however, that Eq.(42) holds in the framework of the linear approximation, which becomes worse for strongly recombining grain boundaries.

Discussion and Conclusion

It has been shown that the concept of charge collection probability allows a common description of different EBIC experiments and also suggests new possibilities of evaluating the related measurements. The approach has been mainly mathematical and obviously has the limits of the underlying physical scheme. In fact, there are experimental results which are beyond the description possibilities of the basic charge-collection model employed here.

For instance, low injection conditions have been assumed throughout; these conditions are met in most experiments, but there is evidence for injection-dependent effects both in the bulk and at the surface of semiconductors (Davidson et al., 1982). Similarly, an influence of the injection level on the EBIC images of defects has been observed (Kittler, 1980), (Leamy, 1982), (Wilshaw and Booker, 1985).

A further limit of the present discussion is related to the depletion layer. Its presence has been described with the boundary condition $\varphi = 1$ at the edge, if the excitation occurs in the neutral semiconductor, or with a condition of complete collection ($\varphi=1$ in the depleted region) when the charge collected in the depletion region is substantial. These approximations do not allow a description of the contrast of defects lying in the depleted region and the related field-dependent effects (Kittler, 1980), (Leamy, 1982), (Toth, 1985). Actually, the most detailed characterization of the electrical activity of dislocations has been performed on defects lying in a neutral region, where the description of the contrast formation in terms of pure diffusion of carriers is adequate (Pasemann et al., 1982), (Wilshaw and Booker, 1985).

Recently, however, recombination at line defects lying, at least in part, in the depletion layer, has been described by attributing to the defect an effective radius ε dependent on the defect position in the depletion layer (Joy and Pimentel, 1985), (Sieber, 1987). Thus the recombination strength of the defect γ_d becomes dependent on this position, since $\gamma_d \propto \varepsilon^2$. A different possibility would be to keep the geometrical features of the defect unchanged and introduce a dependence of γ_d on the electric field.

In conclusion, making the basic contrast model more adherent to the observed recombination effects requires extending the dependence of $\varphi(\underline{r})$, both in the bulk and at defects, on additional physical parameters, as the injection level, the electric field or the temperature.

Acknowledgments

This work was performed with a partial contribution of CNR - Progetto Finalizzato Materiali e Dispositivi per l'Elettronica.

References

Berz F, Kuiken HK (1976) Theory of life time measurements with the scanning electron microscope: steady state. Solid-State Electronics 19, 437-445.

Davidson SM, Innes RM, Lindsay SM (1982) Injection and doping dependence of SEM and scanning light spot diffusion length measurements in silicon power rectifiers. Solid-State Electronics 25, 261-272.

Donolato C (1978/79) On the theory of SEM charge-collection imaging of localized defects in semiconductors. Optik 52, 19-36.

Donolato C (1979) Contrast formation in SEM charge-collection images of semiconductor defects. Scanning Electron Microsc. 1979;I 257-266.

Donolato C (1983a) Evaluation of diffusion lengths and surface recombination velocities from electron beam induced current scans. Appl.Phys. Lett. 43, 120-122.

Donolato C (1983b) Theory of beam induced current characterization of grain boundaries in polycrystalline solar cells. J.Appl.Phys. 54, 1314-1322.

Donolato C (1985a) A reciprocity theorem for charge collection. Appl.Phys.Lett. 46, 270- 272.

Donolato C (1985b) Charge collection in a Schottky diode as a mixed boundary-value problem. Solid-State Electronics 28, 1143-1151.

Donolato C (1986a) An inverse problem of charge-collection microscopy. Inverse Problems 2, L31-34.

Donolato C (1986b) On the temperature dependence of the EBIC contrast of dislocations. J. Physique 47, 171-173.

Donolato C, Kittler M (1987) Depth profiling of the minority-carrier diffusion length in intrinsically gettered silicon by electron-beam-induced current. J.Appl.Phys. (in press).

Everhart TE, Hoff PH (1971) Determination of kilovolt electron energy dissipation vs penetration distance in solid materials. J.Appl.Phys. 42, 5837-5848.

Fuyuki T, Matsunami H, Tanaka T (1980) The influence of the generation volume of minority carriers on EBIC. J.Phys.D: Appl.Phys. 13, 1093-1100.

Hackett WH (1972) Electron-beam excited minority-carrier diffusion profiles in semiconductors. J.Appl.Phys. 43, 1649-1654.

Hanoka JI, Bell RO (1981) Electron-beam-induced currents in semiconductors. Ann.Rev.Mater. Sci. 11, 353-380.

Holt DB, Lesniak M (1985) Recent developments in electrical microcharacterization using the charge-collection mode of the scanning electron microscope. Scanning Electron Microsc. 1985; I: 67-86.

Ioannou DE (1980) A SEM-EBIC minority-carrier lifetime-measurement technique. J.Phys.D: Appl.Phys. 13, 611-616.

Ioannou DE, Dimitriadis CA (1982) A SEM-EBIC minority-carrier diffusion length measurement technique. IEEE Trans.Electron Devices ED-29, 445-450.

Jackson JD (1975) Classical Electrodynamics. J.Wiley, New York, p.51.

Joy DC, Pimentel CA (1985) Quantitative EBIC imaging by Monte Carlo simulation. In: Microscopy of semiconducting materials 1985. Conf.Ser.No.60, Cullis AG, Holt DB (eds.), Institute of Physics, Bristol and Boston, 355-360.

Kittler M (1980) On the characterization of electrically active inhomogeneities in semiconductor silicon by charge collection at Schottky barriers using the SEM-EBIC (II). Kristall und Technik 15, 575-584.

Kittler M, Schröder KW (1983) Determination of semiconductor parameters and the vertical structure of devices by numerical analysis of energy-dependent EBIC measurements. Phys.Stat. Sol. (a)77, 139-151.

Kittler M, Schröder KW, Bugiel E, Becker C (1984) Quantitative EBIC investigations on bulk stacking faults in silicon. Phys.Stat.Sol. (a)81, K131-135.

Kuiken HK, van Opdorp C (1985) Evaluation of diffusion length and surface recombination velocity from a planar-collector-geometry electron-beam-induced current scan. J.Appl.Phys. 57, 2077-2090.

Leamy HJ (1982) Charge collection scanning electron microscopy. J.Appl.Phys. 53, R51-80.

Luke KL, von Roos O, Cheng LJ (1985) Quantification of the effects of generation volume, surface recombination velocity, and diffusion length on the electron-beam-induced current and its derivative: determination of diffusion lengths in the low micron and submicron ranges. J.Appl.Phys. 57, 1978-1984.

Mil'vidskii MG, Osvenskii VB, Reznik VYa, Shershakov AN (1985) Determination of recombination activity and depth of point-like defects in semiconductor crystals by the method of an induced current in a scanning electron microscope. Sov.Phys. Semiconductors 19, 22-25.

Misiakos K, Lindholm FA (1985) Generalized reciprocity theorem for semiconductor devices. J.Appl.Phys. 58, 4743-4744.

Morse PM, Feshbach H (1953) Methods of Theoretical Physics. McGraw-Hill, New York, 812-814.

Nauka K, Lagowski J, Gatos HC, Ueda O (1986) New intrinsic gettering process in silicon based on interactions of silicon interstitials. J.Appl. Phys. 60, 615-621.

Oelgart G, Fiddicke J, Reulke R (1981) Investigation of minority-carrier diffusion lengths by means of the scanning electron microprobe (SEM). Phys.Stat.Sol. (a)66, 283-292.

Ourmazd A, Wilshaw PR, Booker GR (1983) The temperature dependence of the EBIC contrast from individual dislocations in silicon. J.Physique Coll. 44(C4), 289-295.

Pasemann L (1981) A contribution to the theory of the EBIC contrast of lattice defects in semiconductors. Ultramicroscopy 6, 237-250.

Pasemann L, Blumtritt H, Gleichmann R (1982) Interpretation of the EBIC contrast of dislocations in silicon. Phys.Stat.Sol. (a)70, 197-209.

Pasemann L (1986) On EBIC and CL contrast from an individual dislocation. Fifth International Symposium on Structure and Properties of Dislocations in Semiconductors. Moscow 17-22 March 1986. Institute of Solid-State Physics, Moscow. Abstract p.99.

Possin GE, Kirkpatrick CG (1979) Electron beam depth profiling in semiconductors. Scanning Electron Microsc. 1979; I: 245-256.

Sieber B (1987) EBIC contrast of defects in cadmium telluride (II). Phil.Mag. B55, 585-598.

Toth AL (1985) Investigation of plasma effect on EBIC dislocation contrast in Si. In: Microscopy of semiconducting materials 1985. Conf.Ser.No.60, Cullis AG, Holt DB (eds.), Institute of Physics, Bristol and Boston, 361-364.

Wilshaw PR, Booker GR (1985) New results and an interpretation for SEM-EBIC contrast arising from individual dislocations in silicon. In: Microscopy of semiconducting materials 1985. Conf.Ser.No.60, Cullis AG, Holt DB (eds.), Institute of Physics, Bristol and Boston, 329-336.

Wu CJ, Wittry DB (1978) Investigation of minority-carrier diffusion lengths by electron bombardment of Schottky barriers. J.Appl.Phys. 49, 2827-2836.

Discussion with Reviewers

D.E.Ioannou: Is the concept of charge-collection probability useful also in the case of transient EBIC measurements?

Author: Yes. The notion of charge-collection probability can simplify the modeling of transient EBIC experiments as well, since the related time-dependent diffusion problem can be reconducted to a stationary one by application of the Laplace transform. Let us consider, for instance, the configuration of Fig.1, in which the electron beam is cut off at the time t=0 and the subsequent decay of the current is measured. The distribution of excess minority carriers $p(\underline{r},t)$ is governed by the time-dependent diffusion equation:

$$\nabla^2 p - (1/L^2)\, p = (1/D)\, \frac{\partial p}{\partial t} \qquad (D1)$$

with the boundary conditions $p(x,y,0,t)=0$ and the initial condition $p(\underline{r},0)=p_0(\underline{r})$; $p_0(\underline{r})$ is here the steady-state distribution existing for $t<0$ and is given explicitly in Eq. (3). By introducing the normalized variables $\underline{R}=\underline{r}/L$, $T=t/\tau$ and applying the Laplace transform to Eq.(D1), we obtain:

$$\nabla^2 \hat{P} - (s+1)\, \hat{P} = - P_o(\underline{R}) \qquad (D2)$$

where $\hat{P}=\hat{P}(\underline{R},s)$ is the Laplace transform of $P(\underline{R},T)$; the boundary condition is:

$$\hat{P}(X,Y,0,s) = 0 \qquad (D3)$$

The problem thus obtained is a three-dimensional, stationary diffusion problem with an extended source. The analogous of the charge-collection probability of Eq.(5) is given by the function:

$$\hat{\varphi}(Z,s) = \exp\left[-(s+1)^{1/2} Z\right] \qquad (D4)$$

which represents the Laplace transform of the current pulse due to an instantaneous unit point source at a depth Z. The Laplace transform of the induced current, similarly to Eq.(9), is given by:

$$\hat{I}(Z_o,s) = \int_0^\infty \hat{\varphi}(Z,s)\, H_o(Z,Z_o)\, dZ \qquad (D5)$$

where $H_0(Z,Z_0)$ is the function resulting from the integration of P_0 with respect to X,Y, and is the same as the one-dimensional Green's function of Eq.(39). The evaluation of the integral of Eq.(D5) yields finally:

$$\hat{I}(Z_o,s) = \frac{1}{s}\left\{\exp[-Z_o] - \exp[-(s+1)^{1/2} Z_o]\right\} \qquad (D6)$$

The inverse transform of this function, i.e. the induced current decay $I(Z_0,T)$, can be obtained from the tables of Laplace transforms and reproduces the expressions given by (Berz and Kuiken, 1976) and (Ioannou, 1980).

D.Köhler: This paper discusses different methods to measure the diffusion and the surface recombination velocity. Is it possible to estimate the error caused by the assumptions of the physical model (no electric field, low excitation, ...)?

Author: It is generally difficult to estimate the errors that arise from a given simplifying assumption, because the problem without that assumption may become untractable. The influence of the injection level on the measurement of L and v_s, with the configuration of Fig.2, has been discussed with some simplifications by (Berz and Kuiken, 1976) and (Davidson et al., 1982); the experimental results of this latter paper show that high excitation increases L, reduced v_s and also causes narrowing of the depletion region. In practice, it is convenient to test for low injection conditions by changing the injection level (i.e. beam energy and current) and checking whether the values of L and v_s are unaffected. Injection-dependent contrast effects at defects are discussed in a recent review (A Jakubowicz (1987) Theory of electron beam induced current and cathodoluminescence contrasts from structural defects of semiconductor crystals: steady-state and time-resolved problems. Scanning Microsc. 1, 515-533).

The presence of a field region with significant thickness (the depletion layer) is actually taken into account in one-dimensional collection efficiency measurements (Fig.3), but is generally neglected in the two-dimensional configuration of Fig.2. This latter simplification, for instance, makes the specification of the origin of the scan somewhat uncertain; an estimate of the consequent error of L and v_s in a particular case is given in (Donolato, 1983a).